

# Rapid prototyping method for 3D PDMS microfluidic devices using a red femtosecond laser

Saadat, Mozafar; Taylor, Marie; Hughes, Arran; Hajjiyavand, Amir M.

DOI:

[10.1177/1687814020982713](https://doi.org/10.1177/1687814020982713)

License:

Creative Commons: Attribution (CC BY)

*Document Version*

Publisher's PDF, also known as Version of record

*Citation for published version (Harvard):*

Saadat, M, Taylor, M, Hughes, A & Hajjiyavand, AM 2020, 'Rapid prototyping method for 3D PDMS microfluidic devices using a red femtosecond laser', *Advances in Mechanical Engineering*, vol. 12, no. 12, pp. 1-12.  
<https://doi.org/10.1177/1687814020982713>

[Link to publication on Research at Birmingham portal](#)

## General rights

Unless a licence is specified above, all rights (including copyright and moral rights) in this document are retained by the authors and/or the copyright holders. The express permission of the copyright holder must be obtained for any use of this material other than for purposes permitted by law.

- Users may freely distribute the URL that is used to identify this publication.
- Users may download and/or print one copy of the publication from the University of Birmingham research portal for the purpose of private study or non-commercial research.
- User may use extracts from the document in line with the concept of 'fair dealing' under the Copyright, Designs and Patents Act 1988 (?)
- Users may not further distribute the material nor use it for the purposes of commercial gain.

Where a licence is displayed above, please note the terms and conditions of the licence govern your use of this document.

When citing, please reference the published version.

## Take down policy

While the University of Birmingham exercises care and attention in making items available there are rare occasions when an item has been uploaded in error or has been deemed to be commercially or otherwise sensitive.

If you believe that this is the case for this document, please contact [UBIRA@lists.bham.ac.uk](mailto:UBIRA@lists.bham.ac.uk) providing details and we will remove access to the work immediately and investigate.

# Rapid prototyping method for 3D PDMS microfluidic devices using a red femtosecond laser

Mozafar Saadat, Marie Taylor, Arran Hughes  and Amir M Hajiyavand

## Abstract

A rapid prototyping technique is demonstrated which uses a red femtosecond laser to produce a metallic mould which is then directly used for the replica moulding of PDMS. The manufacturing process can be completed in less than 6 h making it a viable technique for testing new designs quickly. The technique is validated by creating a microfluidic device with channels of height and depth of 300  $\mu\text{m}$ , with a ramp test structure where the height and width of the channels reduces to 100  $\mu\text{m}$  to demonstrate the techniques 3D capabilities. The resulting PDMS device was easily removed from the metallic mould and closely replicated the shape aside the expected shrinkage during thermal curing. As the technique uses a single replica process, the surface roughness at the base of the channels corresponds to the un-ablated polished metal mould, resulting in a very low surface roughness of 0.361 nm. The ablated metallic mould surface corresponds to the top of the PDMS device, which is bonded to glass and does not affect the flow within the channels, reducing the need for optimisation of laser parameters. Finally, the device is validated by demonstrating laminar flow with the no-slip condition.

## Keywords

Microfluidics, micromanufacture, laser, rapid prototyping, 3D microfluidic chip, lithography

Date received: 11 June 2020; accepted: 1 December 2020

Handling editor: James Baldwin

## Introduction

Manufacturing of microfluidic devices is performed using a variety of lithography methods including photolithography and soft lithography. Photolithography allows for patterning of features with a high resolution (1  $\mu\text{m}$  under standard conditions), however it requires expensive equipment, a clean room, training and often hazardous substances. Soft lithography is a technique where elastomeric stamps or moulds are used to generate the desired features on a substrate.<sup>1</sup> This method also allows for high resolution (down to 30 nm), however the manufacturing of the initial elastomeric stamp/mould requires microlithographic methods (either photolithography or micromachining). Usually, elastomeric stamps are made from polydimethylsiloxane

(PDMS) or polymethylmethacrylate (PMMA). PDMS has gained significant interest in the scientific field not only for the manufacturing via soft lithography but also as the final material in microfluidic devices. PDMS has many desirable properties for use in microfluidics, such as inertness, biocompatibility (non-toxicity), porous to allow oxygen to diffuse through for live cells, optical

---

Department of Mechanical Engineering, School of Engineering, University of Birmingham, Birmingham, UK

### Corresponding author:

Arran Hughes, Department of Mechanical Engineering, School of Engineering, University of Birmingham, Edgbaston, Birmingham, West Midlands B15 2TT, UK.  
Email: ajh345@bham.ac.uk



transparency (at 230–700 nm), flexibility and stability at a wide range of temperatures.<sup>2–4</sup> It is also cheap, and many manufacturing methods allow for rapid prototyping using PDMS: making it very suitable for the production of low cost, single use (disposable) devices required for research. There are, however, some disadvantages associated with PDMS particularly within the biomedical field such as evaporation occurring within the channels leading to air bubble propagation which can lead to cell death or the high absorption of hydrophobic compounds however these problems can be mitigated through the use of certain surface coatings (such as parylene to prevent absorption) or environment control (such as humidifying the environment to prevent evaporation).<sup>5</sup>

Replica moulding is a well-established technique for producing microfluidic devices, which is low cost and requires little specialist equipment.<sup>6–8</sup> It involves pouring unpolymerised PDMS and a curing agent onto a mould and thermally curing the PDMS in an oven. The cured PDMS can then be peeled from the mould to give the microfluidic device. A clean room environment is not required and the equipment is cheap. The mould used for the fabrication of the microfluidics device is usually made from Su-8 or PDMS which is in-turn produced using conventional (and expensive) photolithographic techniques. There has also, however, been more interest in the direct writing of PDMS utilising laser engraving as opposed to utilising photolithographic techniques.<sup>9</sup> In recent years there has been increasing interest in using metal as the mould for the replica moulding of PDMS. Metallic moulds have advantages over conventional material moulds; as they can withstand the high temperatures with little expansion during thermal curing due to low thermal coefficients of expansion and can be re-used many times.<sup>10</sup> Demoulding of PDMS from metallic moulds has also been performed successfully without the need for surface coatings, further increasing the appeal of metallic moulds.<sup>11–13</sup>

The use of lasers for the manufacture of metallic moulds has become increasingly popular in recent years. Laser ablation is a non-contact process and can achieve high resolution geometries, limited by the beam spot diameter of the laser optics system. Three main types of lasers can be used: continuous wave, pulsed (nanosecond) or ultra-fast pulsed (femtosecond).<sup>14</sup> Pulsed lasers can give high quality ablation after optimisation of laser optical parameters, which has been widely researched.<sup>15,16</sup> Ultra-fast lasers give the highest quality of surrounding material, due to the laser pulse duration being smaller than the electron cooling time (and lattice heating time) of the material, resulting in the material removal via sublimation rather than more conventional melting and vapourisation.<sup>17</sup>

Currently, the manufacture of microfluidic devices is often costly, complicated, can take a long time and

generally requires a lot of training. A comparison of some of the features for microfluidic device mould manufacture is shown in Table 1.

Additional to Table 1, optimisations of these various techniques have been researched such as with micro-milled channels with gas-blowing assisted PDMS coating which allows for 3D planar surfaces to be manufactured and then optimising the surface by coating it with PDMS however this has only been researched for 100–800  $\mu\text{m}$ .<sup>30</sup> Additional full 3D techniques have also been explored such as the development of three-dimensional microfluidic mixers in glass by femtosecond laser direct writing or other 3D microstructures which are suspended inside fused glass or silica however these techniques don't seem to be suitable for mould manufacture and only generate a single prototype for usage so to create more devices the initial manufacturing must be performed again.<sup>31–34</sup> Laser ablation for moulds has also been discussed previously by Isiksacan et al.<sup>35</sup> however the devices manufactured would require several steps to achieve 3D planar surfaces as the ablation was a through-cut of sacrificial PDMS and acetate. From Table 1, a comparison can be made between each of the manufacturing processes to determine the niche where laser ablation lies.

From Table 2 it can be seen that laser ablation should be used for research prototyping due to the low commercial availability and for those researchers with access to laser facilities as an alternative for outsourcing their manufacturing. The other advantage of this is the relatively low operational costs so researchers entering the field of microfluidics can begin developing designs immediately with a relatively quick manufacturing time. The technology itself is suitable for chip designs with 3D geometries where small features may still be required and developed as seen in our test structure developed below. Finally, due to the laser ablation technique developing a mould, this allows for the development of chips that can be tested in biomedical applications where cleaning the chip is not suitable between each experiment. This therefore allows multiple chips to be developed cheaply using PDMS as prototype testing for developing research microfluidic designs.

Our group proposes a rapid prototyping method which is comparatively fast and simple, as shown from Tables 1 to 2, making it more accessible for research groups who have access to laser facilities as well as offering the option of creating 3D moulds for more complex designs. The method should produce microfluidic devices which can be used for many different applications, from cell manipulation to fluid mixing, or bio-medical reactions (such as DNA micro-arrays) and for our own research, developing microfluidic devices in the field of biological cell injection.

Within this paper, a novel manufacturing method is demonstrated for the rapid prototyping of microfluidic

**Table 1.** A brief summary of current microfluidic mould manufacture techniques.<sup>18–29</sup>

Microfabrication technology	Geometry choice	Minimum feature size	Max height	Time/speed	Cost	Commercial availability
Laser ablation of steel mould	All geometry including 3D (no undercuts)	1 $\mu\text{m}$	1 mm	1 mm/min	Expensive initial capital costs but cheaper operating costs due to no clean-room facilities required	Suitable for 3D prototyping but not commercially due to it being a serial process
Wet etch	2D only	3 $\mu\text{m}$	500 $\mu\text{m}$	1–3 $\mu\text{m}/\text{min}$	Expensive due to clean-room facilities	Most common mould manufacturing technique with high throughput
Dry etch	All geometry including 3D (some undercutting)	100 nm	10 $\mu\text{m}$	100 $\mu\text{m}/\text{min}$	More expensive than wet etch due to plasma generation	Widely used but not as often as wet etching
Deep reactive ion etching	All geometry including 3D (no under cuts)	40–100 nm	500 $\mu\text{m}$	3.2 $\mu\text{m}/\text{min}$	Very expensive due to initial capital	Not often used
E-beam lithography	2D only	1–100 nm	5 $\mu\text{m}$	1–500 nm/min	Most expensive due to capital and operating costs	Ideal for low volume applications only due to no mask requirement
Powder blasting	2D only	<50 $\mu\text{m}$	>1 mm	1 mm/min	Relatively cheap due to not requiring clean room	Not widely used due to being a serial process
Microcutting	All geometry including 3D (no undercuts)	0.1–25 $\mu\text{m}$	40 $\mu\text{m}$	6 mm/min	Expensive due to control and tooling prices	Not widely used due to being a serial process and specialist equipment needed
X-ray lithography (LIGA)	2D only	0.1–3 $\mu\text{m}$	0.1–1 mm	0.24 $\mu\text{m}/\text{min}$	Very expensive due to initial capital and operating costs	Not used often due to specialist equipment/facilities being required
Wax 3D printing	All geometry including 3D	75 $\mu\text{m}$	50 $\mu\text{m}$	Varies as function of channel size	Very cheap due to low initial capital and operating costs	Technology is currently being developed to be used in wider research

devices with 3D structures using a metallic mould, and the subsequent produced device is analysed using the surface roughness of the channels and the geometric difference between the mould and final device is shown. To demonstrate that the manufacturing method can produce devices which are suitable for microfluidic applications, the device is tested to evaluate its capability of maintaining laminar flow within the channels.

## Proposed methodology

### Mould manufacture

The proposed method is fast, and requires only three pieces of specialist equipment; a femtosecond laser, a

vacuum pump and an oven. To the best of our knowledge, this direct replica moulding technique of PDMS using a femtosecond laser is novel and can be used in the future for rapid prototyping of microfluidic devices.

Commercially available 430 grade ferritic stainless steel was used as the material for the metallic moulds. Disks of 50 mm diameter were machined out of plates of thickness 0.7 mm and surface roughness of  $S_a = 0.197 \mu\text{m}$ . A femtosecond pulsed laser (Satsuma from Amplitude Systemes) was used to micro-machine the microfluidic channels (Lasea Multi-Axis Micro Machining Centre). The technical parameters of the laser source are listed in Table 3.

**Table 2.** A comparative summary of each of the manufacturing processes based on Table 1.

Microfabrication technology	Geometry choice	Minimum feature size	Max height	Time/speed	Capital costs	Operational costs	Commercial availability
Laser ablation of steel mould	+	+	+	+	-	+	-
Wet etch	-	-	-	-	+	-	+
Dry etch	+	+	-	-	+	-	+
Deep reactive ion etching	+	+	-	-	-	-	-
E-beam lithography	-	+	-	-	-	-	-
Powder blasting	-	-	+	+	+	+	-
Microcutting	+	+/- (depending on tooling)	-	-	-	-	-
X-ray lithography (LIGA)	-	+	+	-	-	-	-
Wax 3D printing	+	-	-	-	+	+	-

**Table 3.** Laser processing parameters for femtosecond laser used for ablation.

Parameter	Value
Central wavelength, $\lambda$ (nm)	1030
Pulse duration, $\tau_{pulse}$ (fs)	310
Average power, $P_{avg}$ (W)	5
Pulse energy, $E$ ( $\mu$ J)	7
Repetition rate, $f$ (kHz)	500
Beam quality, $M^2$	<1.3

The laser delivery system included a quarter wave plate to convert the s-type linear polarised beam to a circular polarised beam. The beam then passes through a beam expander and is fed into the Galvo-scanner head (RhoTHor RTA). The Galvo-Scanner head includes a telecentric lens and directs the beam onto the sample's surface. The laser spot was Gaussian-shaped with spot diameter  $2\omega_o = 5 \mu\text{m}$  in the focal plane. Assuming  $M^2$  of 1.3, the Rayleigh length  $Z_R$  of the beam can be estimated to be 0.55 mm using,

$$Z_R = \frac{\pi\omega_o^2}{\lambda M^2} \quad (1)$$

where  $\omega_o$  is the beam radius,  $\lambda$  is the wavelength and  $M^2$  is the beam quality of the laser. The microfluidic device was designed in SolidWorks CAD software to have a main channel height and depth of  $300 \mu\text{m}$  with a 3D geometry generated of a ramp which reduces uniformly in height and width to  $100 \mu\text{m}$  to demonstrate the effectiveness of laser manufacturing 3D structures on metallic moulds as shown in Figure 1.

The model shown in Figure 1 highlights all geometric shapes that could be expected in a microfluidic device as well as being able to highlight the 3D capabilities of the device. The CAD model was sliced using the ArtCAM software from AUTOCAD, and machine code generated using the laser control software Kyla. The scanning strategy used was Raster Mode scanning with 4 lines at  $45^\circ$  angles in each layer, with no contouring of the geometry. The hatch distance between each line was  $4 \mu\text{m}$  giving a lateral overlap for each pulse of  $31 \mu\text{m}$ . The scanning speed,  $v$ , was  $750 \text{ mm/s}$ , meaning a pulse separation,  $d$ , of  $1.5 \mu\text{m}$ , which was calculated using equation (2)

$$d = \frac{v}{f} \quad (2)$$

With  $f$  being the repetition rate. 300 layers were required to give a final depth of  $300 \mu\text{m}$ . As the depth of the sample ( $0.3 \text{ mm}$ ) is smaller than the calculated Rayleigh length, the focal point of the laser was kept constant for all layers. The lasing was performed at room temperature and atmospheric pressure with an extractor fan removing debris during ablation. The

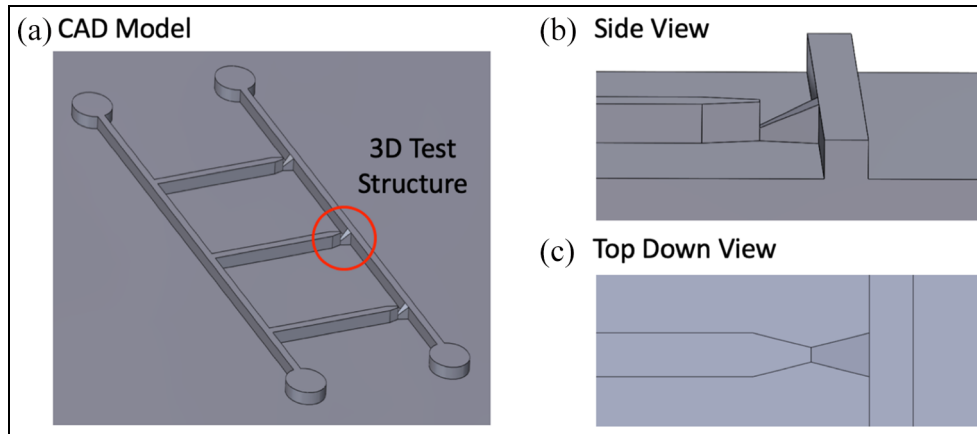


**Figure 1.** (a) CAD model of a test microfluidic device with channel heights and widths of  $300\ \mu\text{m}$ , (b) 3D test structure showing a ramp reduction in height to  $100\ \mu\text{m}$  and step back up to  $300\ \mu\text{m}$  and (c) top down view of the 3D test structure showing decreasing width to  $100\ \mu\text{m}$ .



**Figure 2.** View of the stainless steel negative mould for the manufacture of the PDMS channels.

laser processing job took 150 min to complete and a negative mould of the device was made as shown in Figure 2.

### Device manufacture

The PDMS (SYLGARD<sup>®</sup> 184, Dow Corning, MI) was prepared as described by the steps in Figure 3.

Before step 4 in Figure 3 excess PDMS is cut off and channel openings were made using a Whatman Uni-Core 2.00 mm Punch and then cleaned and dried with ethanol. Due to the low weight of the device and small film thickness, the thin layer of PDMS mixture did not squeeze into the channels as no pressure was required to stick the device to the glass slide. The whole process

can be completed in less than 6 h. About 1 h is required for laser system setup, 2.5 h for the mould fabrication via laser ablation, 1.5 h for PDMS preparation and device manufacture via thermal curing and 1 h for sealing the device to a glass plate using PDMS and thermal bonding.

### Device testing

Typical methods to measure the flow velocity within channels include particle image velocimetry, hot wire anemometry or pressure probes.<sup>36–38</sup> Particle image 8 velocimetry is an indirect, non-intrusive technique which uses tracer particles within flow to determine flow velocity and can be applied to micro-geometries. Typically, tracer particles for use in microfluidic devices are small (on the nanoscale) spherical fluorescent beads, and their motion is recorded using epifluorescence microscopes and other optical equipment.<sup>39</sup> In this report, a simplified version of particle image velocimetry is performed using food dye and a high frame rate camera. The aim is to demonstrate that the channels can maintain laminar flow, which is a requirement for most microfluidic devices. This can be done by calculating the maximum flow velocity within the channels and comparing it to theoretical laminar results.

The device was filled with de-ionised water by attaching a syringe to tubing with an outer diameter of 2 mm which was then inserted into one of the inlets of the device. Another syringe was filled with red food colouring and placed in a World Precision Instruments syringe pump, and then connected to the device using tubing. The device was placed in a petri-dish on a BestScope BS-2090 inverted microscope, equipped with a x0.45 Basler 106752 Camera set to record at 200 frames per second (fps). The syringe pump was used to deliver the

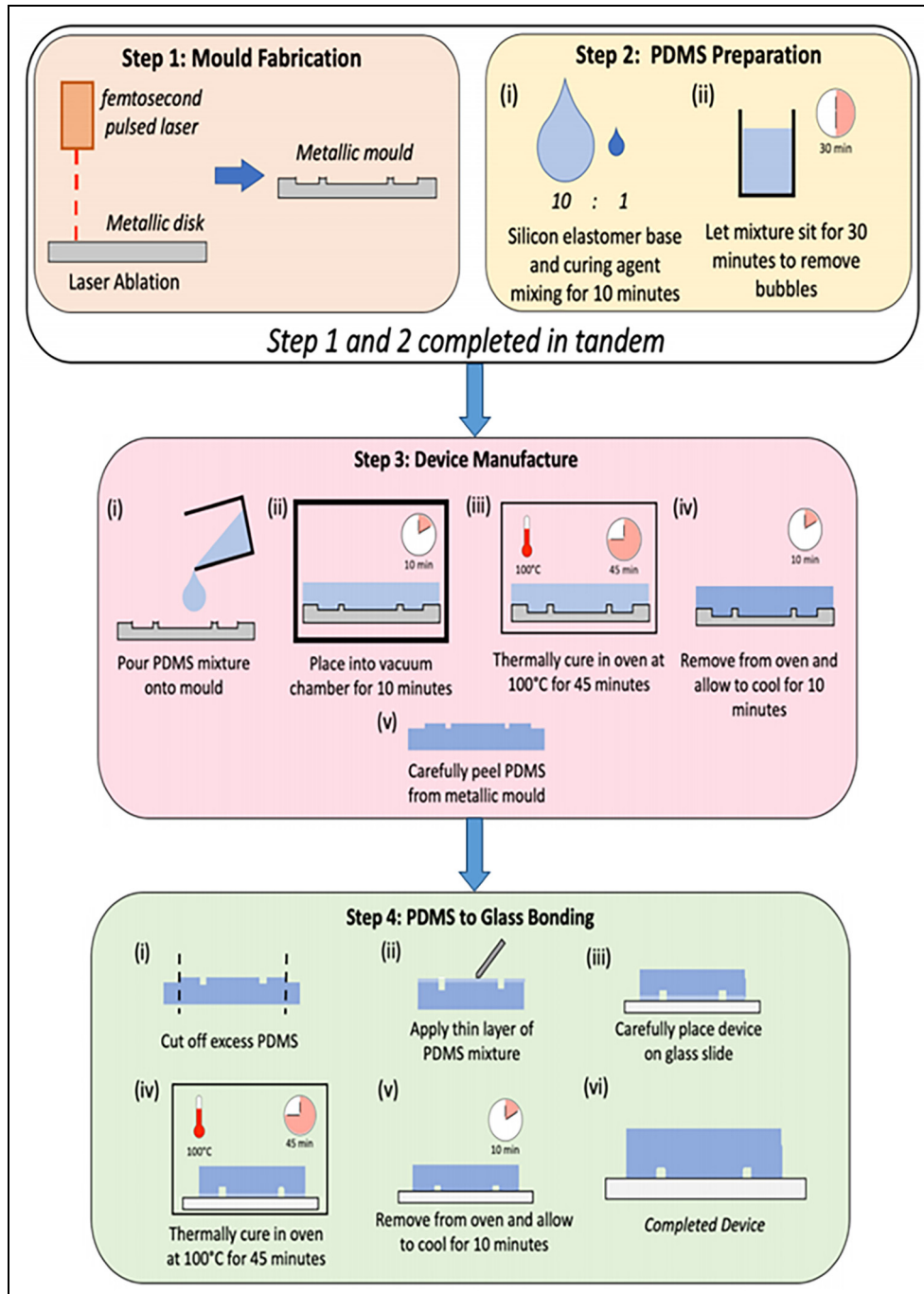


**Figure 3.** Step by step procedure of the manufacture of the PDMS device. Step 1: The mould is fabricated using the femtosecond laser as described above. Step 2: PDMS is prepared by mixing in a 10:1 ratio as recommended by the manufacturer and left to sit. Step 3: PDMS is poured onto the device, vacuumed, thermally cured and then peeled. Step 4: PDMS is bonded to the glass using PDMS as glue then cured for the final device.

dye into the water filled device to estimate the velocity of the water within the channels. Footage was recorded for volumetric flow rates ranging from 0.04 to 0.3 ml/min, between each flow rate reading the device was flushed thoroughly with de-ionised water to remove the dye. The testing was performed at room temperature (19°C) and the set up can be seen in Figure 4.

## Results and discussion

### Analysis of mould and device

The metallic mould and fabricated PDMS device were analysed using an Alicona G4 InfiniteFocus (IF) system to obtain surface roughness and surface profile measurements. Surface roughness measurements were

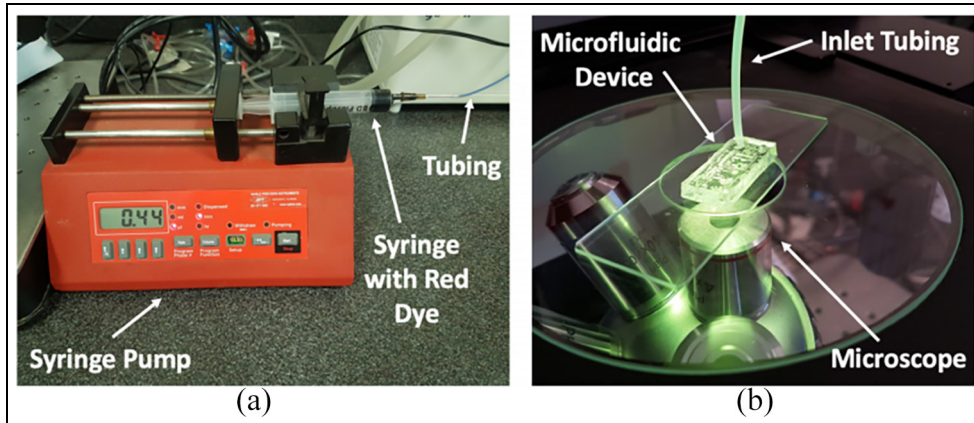


**Figure 4.** (a) Syringe pump to apply constant fluid flow to the device and (b) the microfluidic device under a microscope.

**Table 4.** Surface roughness ( $S_a$ ) values for the mould and device at specific locations.

Position	PDMS	Metal
$S_a$ top surface ( $\mu\text{m}$ )	3.496	2.625
$S_a$ bottom of channel ( $\mu\text{m}$ )	0.361	0.197

taken in two places on both the device and mould: i) the top surface of the device, corresponding to the ablated metal of the mould and ii) the bottom of the channels of the device, corresponding to the polished metal of the mould. The surface roughness values are shown in Table 4.

Similar to the technique performed by the surface roughness at the base of the channels is similar to the surface roughness of the initial polished metal disk.<sup>40</sup> This leads to low surface roughness in the channels of the final device, reducing friction and aiding laminar flow. This also allows the possibility to easily change the surface roughness of the channels, by selecting an initial metal substrate with the desired surface roughness. The surface roughness at the top of the device (corresponding to the ablated metal) is higher, at 3.496 and 2.625  $\mu\text{m}$  for the PDMS and metal mould, respectively. However due to the top-lid design of the microfluidic device, it is thermally bonded to a glass slide and does not affect the flow within the device. This is advantageous as it means that the resulting surface roughness produced by the laser ablation does not need to be greatly optimised as it has little effect on the functionality of the device. The surface roughness has increased by 60.4% and 30.2% from the metal to the PDMS for the top surface and bottom of channel respectively. Profile cross sections of the channel were measured using the Alicona System at locations A and B shown in Figure 5.

Cross section A shows the general cross section of the channel measured and is shown in Figure 6(a). The

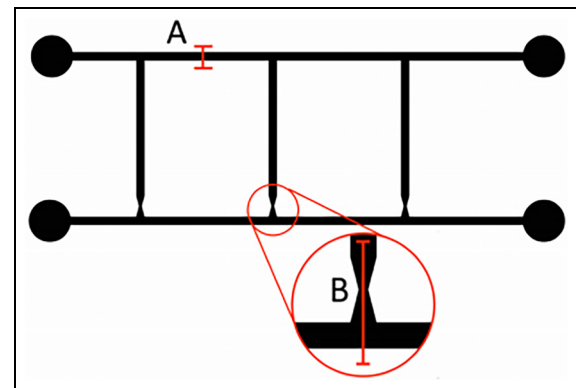


**Figure 5.** Surface profile measurement cross section locations for the device. 'A' corresponding to the general channel cross section. 'B' corresponding to the longitudinal cross section of the 3D test structure.

general shape of the resulting channel in both metal and PDMS shows a narrow bottom, opening up to a wider entrance. This change from narrow to wider side walls is caused by tapering of the laser ablation as it progresses further into the metal. Beam reflection and energy absorption occurs on the side walls and the beam can self-focus in the plasma generated, leading to a lower laser power on the sample. This reduces the fluence of the laser contacting the surface and results in poorer ablation. This effect has been widely researched and can be reduced by varying the optical parameters, such as the laser fluence, or depth of focus (Rayleigh Length) of the laser source.<sup>41</sup>

The metallic mould shows maximum undershoots of 42  $\mu\text{m}$  (Figure 6(a)) at the edges of the channels, which are also replicated in the PDMS, to a lesser extent of 30  $\mu\text{m}$  due to the shrinkage of the PDMS during thermal curing. These undershoots border all channel edges, which can be seen more clearly in Figure 7(b) and are due to the raster scanning strategy of the laser.



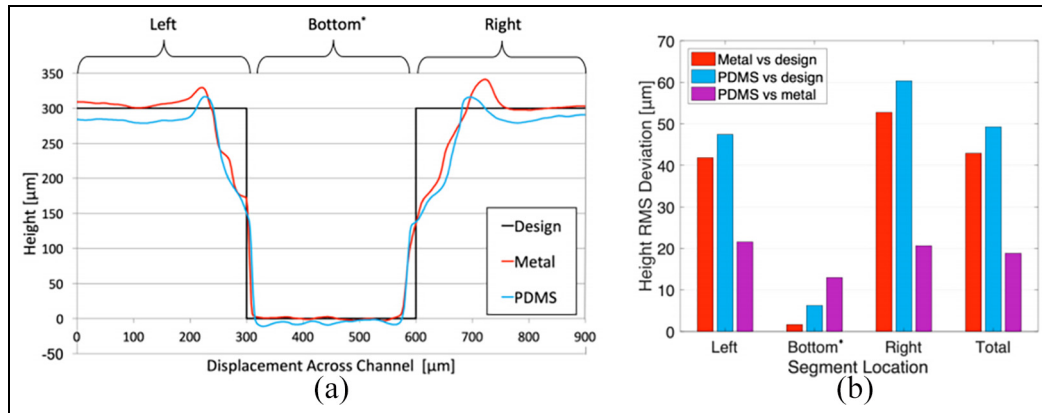


**Figure 6.** (a) Cross section of channels at location (A) from Figure 5 for the metal mould and PDMS device. The PDMS and metal were aligned with their datums set at a height of  $0\ \mu\text{m}$  at the bottom of the channels when taking measurements and (b) the root mean squared (RMS) deviations in the y direction (height) between the desired shape, metal and PDMS at different locations. NB: the bottom location has been truncated  $30\ \mu\text{m}$  on either side, to remove the large errors at the walls of the channels to give a representative RMS along the bottom of the channel.

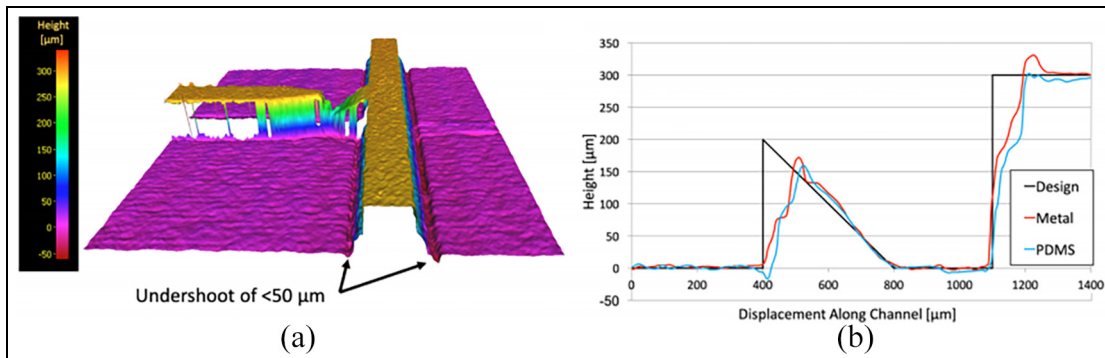


**Figure 7.** (a) 3D height profile of metal mould of the channels including the 3D test structure and (b) longitudinal cross section B of 3D test structure for metal mould and PDMS (see Figure 5).

The laser decelerates then accelerates at the channel edges to change direction and start a new line in the raster scanning mode. This results in more pulses of the laser reaching the surface at these points and hence more ablation occurs at the edges of the channels. It is possible to optimise the scanning strategy to avoid these edge effects, by adding ‘off times’ to the laser during deceleration and direction changes, or by using PID controllers to minimise the errors in the galvanometer’s movement.<sup>42</sup> A standalone software tool has been developed in recent years which causes adjustments to the beam path to avoid effects caused by the difference in the desired and actual beam path due to acceleration and deceleration of the beam.<sup>43</sup> The use of this software would reduce to overshoot effects seen in our sample.

The Root Mean Squared (RMS) deviation of the height of the metal and PDMS compared to the design height are calculated in MATLAB 2017a and shown in Figure 6(b). These have been calculated on the left,

right, bottom and across the whole of the profile. Due to shrinkage of the PDMS during thermal curing, higher RMS values are seen for PDMS than the metal when compared to the design. The RMS for metal and PDMS at the top of the channels is large ( $41.9\text{--}52.7\ \mu\text{m}$  and  $47.5\text{--}60.4\ \mu\text{m}$ , respectively), due to the aforementioned tapering and undershoots. To obtain a true RMS for the bottom of the channel, the results were truncated by  $-30\ \mu\text{m}$  on either side of the channel walls to remove the large errors seen on the channel walls. Here we see small RMS values ( $1.68\ \mu\text{m}$  and  $6.3\ \mu\text{m}$  respectively) compared to the desired shape. In total across the channel profile, the RMS for metal and PDMS is  $42.9$  and  $49.3\ \mu\text{m}$ , respectively, which, though large, it is clear that with laser parameter optimisation these RMS values can be greatly improved.

The RMS is also calculated between the metal and PDMS to evaluate the changes in the PDMS during curing. Across the channel profile, the total RMS between the metal and the PDMS is  $18.8\ \mu\text{m}$ , due to

shrinkage during thermal curing. PDMS shrinkage has widely been researched and is affected by the ratio of curing agent to elastomer base and the curing temperature and time.<sup>7</sup> Using the calculated RMS (or expected % shrinkage of PDMS from tables), the metal mould can be re-designed to negate the effects of the shrinkage and hence better replicate the desired geometry.

The 3D test structure in the channels is also examined. Figure 7(a) shows a 3D height profile of the metallic mould at the restriction and the cross section of the change in height of the channels across the restriction (B in Figure 5). The horizontal accuracy of the metallic mould and resulting PDMS at the base of the channels (height 0  $\mu\text{m}$ ) is good, with the test structure starting and ending within  $\pm 20 \mu\text{m}$  of the correct location. The tip of the structure is intended to be a vertical surface reaching to 200  $\mu\text{m}$  however the metal and PDMS have failed to do this. The metal mould has undershot the height by 28  $\mu\text{m}$  and has a horizontal error of 110  $\mu\text{m}$ , and the PDMS closely replicates this with errors of 40 and 122  $\mu\text{m}$ , respectively. These large errors are due to the minor level of optimisation of the laser parameters and scanning strategy, and could be improved as discussed previously. However, the resulting PDMS device has successfully replicated 3D structures within the micro-channels.

### Laminar flow

The transition from laminar to turbulent flow in channels typically occurs at Reynolds numbers over 2000. The maximum flow velocity within our channels for laminar flow can be calculated using equation (3):

$$Re = \frac{\rho u D_h}{\mu} \quad (3)$$

Where  $\rho$  is the density of the fluid,  $u$  is the average fluid velocity,  $\mu$  is the dynamic viscosity of the fluid and  $D_h$

is the hydraulic diameter of the channel which for rectangular channels is calculated as

$$D_h = \frac{4A}{C} \quad (4)$$

Where  $A$  is the cross-sectional area of the channel and  $C$  is the wetted perimeter of the channel. This yields a maximum mean inlet velocity of 7.02 m/s. For laminar flow driven by a constant pressure gradient,  $P$ , the velocity profile of subsequent laminar flow can be calculated using the well-known Hagen–Poiseuille equation. This can be modified for use in rectangular channels with widths  $-\frac{w}{2} < y < \frac{w}{2}$  and heights  $0 < z < h$  yielding

$$u(y, z) = \frac{4h^2 P}{\pi^3 \mu} \sum_{n=1,3,5,\dots}^{\infty} \frac{1}{n^3} \left[ 1 - \frac{\cosh(n\pi \frac{y}{h})}{\cosh(n\pi \frac{w}{2h})} \right] \sin\left(n\pi \frac{z}{h}\right) \quad (5)$$

The volumetric flow rate ( $Q$ ) can be calculated by integrating over the velocity profile yielding

$$Q = 2 \int_0^{\frac{1}{2}w} \int_0^h u(y, z) dy dz = \frac{wh^3 P}{12\mu} \left[ 1 - \sum_{n=1,3,5,\dots}^{\infty} \frac{1}{n^5} \frac{192h}{\pi^5 w} \tanh(n\pi \frac{w}{2h}) \right] \quad (6)$$

By rearranging equation (6) and using the known volumetric flow rate of the fluid the pressure gradient across the channel can be calculated in MATLAB 2017a up to terms  $n = 20$  (higher values only change the eighth decimal place). Using this value, the velocity profile is calculated using equation (5) where the terms converge again at approximately  $n = 20$ . The generated velocity profile for a volumetric flow rate of 0.15 ml/min can be seen in Figure 8 and shows a parabolic profile with a

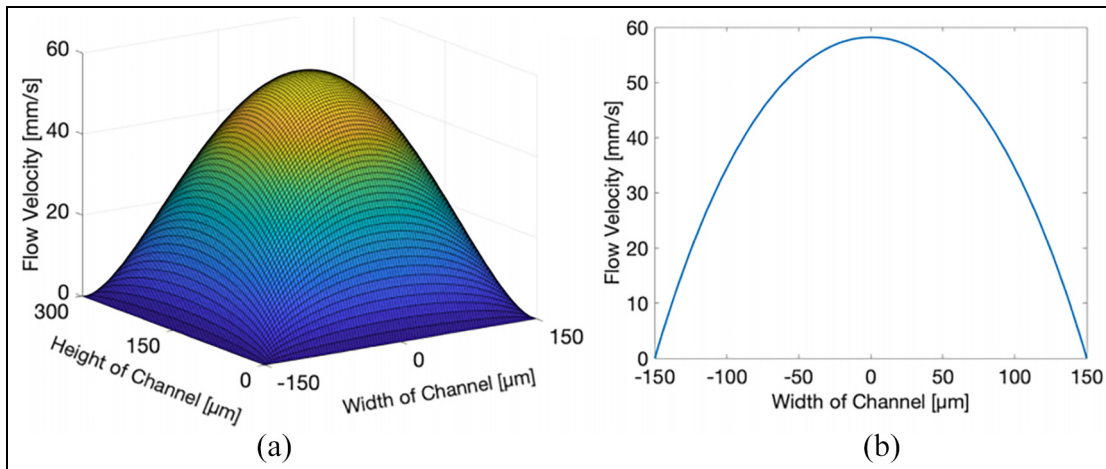


**Figure 8.** (a) 3D and (b) 2D theoretical velocity profile for volumetric flow rate of 0.15 ml/min for laminar flow for channels of height and width of 300  $\mu\text{m}$  based on equation (5).

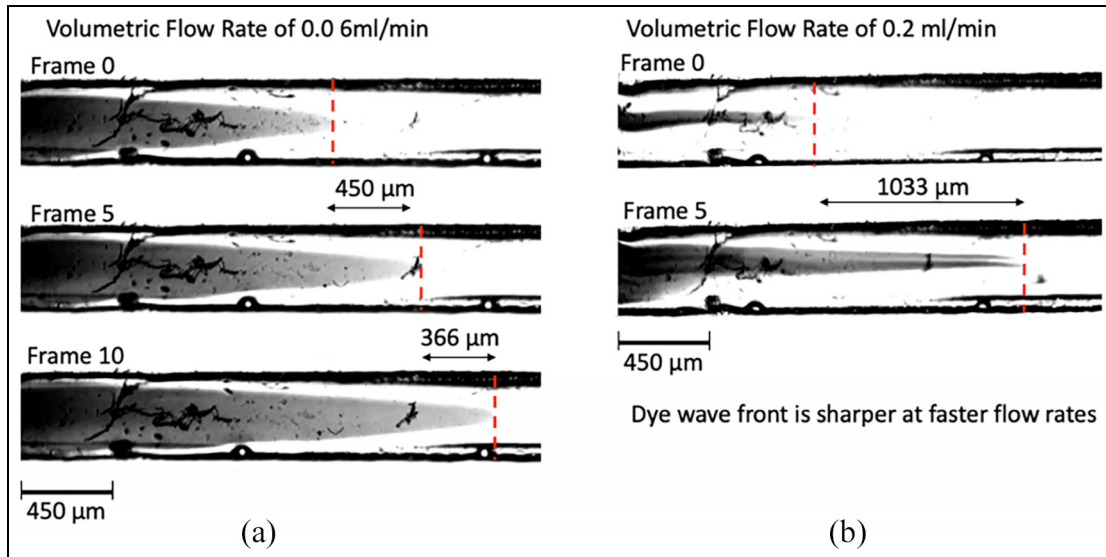


**Figure 9.** Images of the recorded footage of dye flow in the channels: (a) volumetric flow rate of 0.06 ml/min shows a good parabolic flow profile and no-slip condition of the dye at the channel edges and (b) volumetric flow rate of 0.2 ml/min shows a stretched dye profile which is irregular and pointy.

maximum peak velocity of 58.2 mm/s and no-slip condition at the channel walls.

By analysing the recorded footage of the fluid within the channels, the peak velocity of the dye within the channels can be estimated. This was done by measuring the number of frames required for the peak of the dye flow to cover a measured distance and using the known fps of the footage, and can be seen in Figure 9. For lower volumetric flow rates, the dye flow profile was parabolic, and demonstrated the no-slip condition at the channel walls where the dye progressed very little compared to the peak of the flow. The flow also appears un-disturbed and is not showing any turbulence or eddies. For higher flow rates the dye flow profile is much more elongated and irregular (see Figure 9(b)), however there are not any vortices and still the flow still appears to have straight flow lines, as expected for laminar flow.

The maximum velocity of the dye flow is calculated for each of the volumetric flow rates and plotted with the theoretical maximum velocities in Figure 10. A least squares fit has been plotted for the measured data points and has an  $R^2$  of 0.95 showing a strong linear correlation. The experimental results consistently underestimate the maximum flow velocity in the channels which can be attributed to systematic errors such as the channels being larger than the dimensions used in theoretical ones used (see Figure 6(a)) which reduces the flow rate. Another reason could be due to the different sizes of particles of the dye causing it to move slower than the fluid is as it is reliant on the drag force.

In summary, although the results are underestimating the maximum flow velocity within the

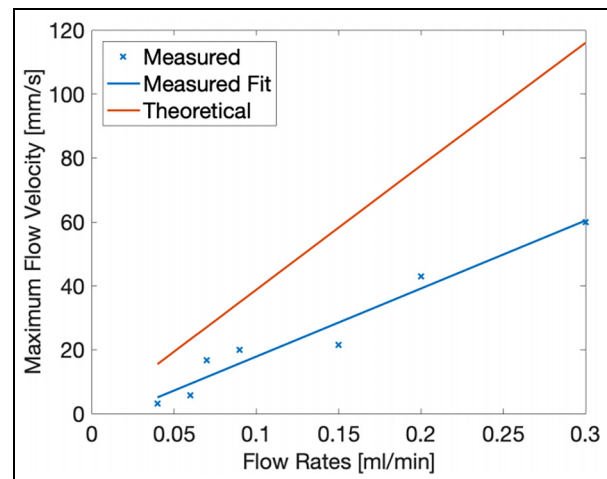


**Figure 10.** Theoretical and measured maximum velocity of flow within the microchannels. A least squares fit has been plotted for the measured results with an  $R^2$  value of 0.95.

channels, the flow profile is laminar due to the parabolic flow shown at lower flow rates, a similar increase in maximum flow velocities for each flow rate and demonstrates the no-slip condition at the channel walls. For higher flow rates, the flow is still laminar due to the lack of vortices and conical, albeit elongated, flow profile demonstrated. This confirms the manufacturing techniques ability to produce channels which can sustain laminar flow. In addition, the produced device remained fully sealed for the entirety of testing which included flushing with de-ionised water and dye over 50 times reflecting the viability and durability of using

uncured PDMS for sealing rather than the conventional plasma bonding.

## Conclusion

A novel rapid prototyping technique for the production of microfluidic devices using a red femtosecond laser was successfully demonstrated. This new method offers a quick way for researchers to generate a microfluidic mould quickly if they have access to laser ablation facilities but not traditional microfluidic manufacturing. The produced device showed low surface roughness at the base of the channels due to the inverse design of the metallic mould. Widening and overshoots at channel cross sections were observed and were attributed to low levels of laser parameter optimisation. A simplified form of particle image velocimetry was used to successfully demonstrate laminar flow within the channels validating the manufacturing method's ability to create microfluidic channels. The quality of the produced device is greatly affected by the quality of the metallic mould. It is clear that with more optimisation of laser micro-processing by minimising impact of the raster scanning for better replication of 3D features, optimising the laser fluence for minimised tapering of the channel walls and implementing sharper laser movement control, this manufacturing technique could be used to create high quality microfluidic devices.

## Acknowledgements

The authors wish to thank with appreciation the laser-based manufacturing research group within the Advanced [M]anufacturing Technology Centre, Department of Mechanical Engineering, University of Birmingham, for the support provided in the manufacturing realisation aspects of this research.


## Declaration of conflicting interests

The author(s) declared no potential conflicts of interest with respect to the research, authorship, and/or publication of this article.

## Funding

The author(s) received no financial support for the research, authorship, and/or publication of this article.

## ORCID iD

Arran Hughes  <https://orcid.org/0000-0002-5159-1424>

## References

- Xia Y and Whitesides GM. Soft lithography. *Annu Rev Mater Sci* 1998; 28: 153–184.
- Zhou J, Ellis AV and Voelcker NH. Recent developments in PDMS surface modification for microfluidic devices. *Electrophoresis* 2010; 31: 2–16.
- Mata A, Fleischman AJ and Roy S. Characterization of polydimethylsiloxane (PDMS) properties for biomedical micro/nanosystems. *Biomed Microdev* 2005; 7: 281–293.
- Berthier E, Young EWK and Beebe D. Engineers are from PDMS-land, biologists are from polystyrenia. *Lab Chip* 2012; 12: 1224–1237.
- Xia Y, McClelland JJ, Gupta R, et al. Replica molding using polymeric materials: a practical step toward nanomanufacturing. *Adv Mater* 1997; 9: 147–149.
- Shih TK, Chen CF, Ho JR, et al. Fabrication of PDMS (polydimethylsiloxane) microlens and diffuser using replica molding. *Microelectron Eng* 2006; 83: 2499–2503.
- Madsen MH, Feidenhansl NA, Hansen P, et al. Accounting for PDMS shrinkage when replicating structures. *J Micromech Microeng* 2014; 24: 127002.
- Hupert M, Guy W, Llopis S, et al. Evaluation of micro-milled mold masters for the replication of microchip electrophoresis devices. *Microfluid Nanofluid* 2007; 3: 1–11.
- Da Costa ET, Mora MF, Willis PA, et al. Getting started with open-hardware: development and control of microfluidic devices. *Electrophoresis* 2014; 35: 2370–2377.
- Chen P and Wang Z. A rapid and low-cost manufacturing for polymeric microfluidic devices. *Adv Mater Res* 2012; 579: 348–356.
- Shiu PP, Knopf GK, Ostojic M, et al. Rapid fabrication of micromolds for polymeric microfluidic devices. In: *Canadian conference on electrical and computer engineering*, Vancouver, 2007, pp.8–11.
- Wu CH, Chen CW, Kuo L, et al. A novel approach to measure the hydraulic capacitance of a microfluidic membrane pump. *Adv Mater Sci Eng* 2014; 2014: 1–9.
- Chichkov BN, Momma C, Nolte S, et al. Femtosecond, picosecond and nanosecond laser ablation of solids. *Appl Phys Mater Sci Process* 1996; 63: 109–115.
- Lauer B, Jäggi B and Neuenschwander B. Influence of the pulse duration onto the material removal rate and machining quality for different types of steel. *Phys Procedia* 2014; 56: 963–972.
- Rousseau A, Laur V, Députier S, et al. Influence of substrate on the pulsed laser deposition growth and microwave behaviour of KTaO<sub>3</sub>. 6NbO<sub>3</sub> 4O<sub>3</sub> potassium tantalate niobate ferroelectric thin films. *Thin Solid Films* 2008; 516: 4882–4888.
- Dubey AK and Yadava V. Multi-objective optimisation of laser beam cutting process. *Opt Laser Technol* 2008; 40: 562–570.
- Petkov PV, Dimov SS, Minev RM, et al. Laser milling: pulse duration effects on surface integrity. *Proc Inst Mech Eng Part B J Eng Manuf* 2008; 222: 35–45.
- Mata A, Fleischman A and Roy S. Fabrication of multi-layer SU-8 microstructures. *J Micromech Microeng* 2006; 16: 276–284.
- Xu J, Locascio L, Gaitan M, et al. Room-temperature imprinting method for plastic microchannel fabrication. *Anal Chem* 2000; 72: 1930–1933.

20. Fiorini G and Chiu D. Disposable microfluidic devices: fabrication, function, and application. *Biotechniques* 2005; 38: 429–446.
21. Li Y, Zhang H, Yang R, et al. In-plane silicon microneedles with open capillary microfluidic networks by deep reactive ion etching and sacrificial layer based sharpening. *Sens Actuators A Phys* 2019; 292: 149–157.
22. Williams K, Gupta K and Wasilik M. Etch rates for micromachining processing-part II. *J Microelectromech Syst* 2003; 12: 761–778.
23. Wensink H. *Fabrication of microstructures by powder blasting*. Enshede, The Netherlands: University of Twente, 2002.
24. Nguyen N. *Micromixers*. 2nd ed. Waltham, MA: William Andrew, 2012, pp.114–153.
25. Laermer F, Franssila S, Sainiemi L, et al. Deep reactive ion etching. In: Tilli M, Motooka T, Airaksinen V, et al. (eds) *Handbook of silicon based MEMS materials and technologies*. Elsevier Inc., 2015, pp.444–469.
26. Muñoz P, Yong YS, Dijkstra M, et al. Double metal layer lift-off process for the robust fabrication of plasmonic nano-antenna arrays on dielectric substrates using e-beam lithography. *Opt Mater Express* 2019; 9: 2046–2056.
27. Xue B, Geng Y, Yan Y, et al. Rapid prototyping of microfluidic chip with burr-free PMMA microchannel fabricated by revolving tip-based micro-cutting. *J Mater Process Technol* 2020; 277: 116468.
28. Chen X and Zhang L. Review in manufacturing methods of nanochannels of bio-nanofluidic chips. *Sens Actuators B Chem* 2018; 254: 648–659.
29. Raoufi MA, Bazaz SR, Niazmand H, et al. Fabrication of unconventional inertial microfluidic channels using wax 3D printing. *Soft Matter* 2020; 16: 2448–2459.
30. Liu X, Dong Z, Zhao Q, et al. Optimization of micro-milled channels for microfluidic applications using gas-blowing-assisted PDMS coating. *Microfluid Nanofluid* 2020; 24: 11.
31. Liao Y, Song J, Li E, et al. Rapid prototyping of three-dimensional microfluidic mixers in glass by femtosecond laser direct writing. *Lab Chip* 2012; 12: 746–749.
32. Kotz F, Risch P, Arnold K, et al. Fabrication of arbitrary three-dimensional suspended hollow microstructures in transparent fused silica glass. *Nat Commun* 2019; 10: 1439.
33. He S, Chen F, Liu K, et al. Fabrication of three-dimensional helical microchannels with arbitrary length and uniform diameter inside fused silica. *Opt Lett* 2012; 37: 3825–3827.
34. LoTurco S, Osellame R, Ramponi R, et al. Hybrid chemical etching of femtosecond laser irradiated structures for engineered microfluidic devices. *J Micromech Microeng* 2013; 23: 085002.
35. Isiksacan Z, Guler MT, Aydogdu B, et al. Rapid fabrication of microfluidic PDMS devices from reusable PDMS molds using laser ablation. *J Micromech Microeng* 2016; 26: 035008.
36. Raffel M, Willert CE, Scarano F, et al. *Particle image velocimetry: a practical guide*. 2nd ed. Springer International Publishing, 2018.
37. Genevieve CB. Hot-wire anemometry. *Annu Rev Fluid Mech* 1976; 8: 209–231.
38. Chue SH. Pressure probes for fluid measurement. *Prog Aerosp Sci* 1975; 16: 147–223.
39. Li H and Olsen MG. MicroPIV measurements of turbulent flow in square microchannels with hydraulic diameters from 200  $\mu\text{m}$  to 640  $\mu\text{m}$ . *Int J Heat Fluid Flow* 2006; 27: 123–134.
40. Shiu PP, Knopf GK, Ostojic M, et al. Non-lithographic fabrication of metallic micromold masters by laser machining and welding. *Int J Adv Manuf Technol* 2012; 59: 157–167.
41. Ravi-Kumar S, Lies B, Zhang X, et al. Laser ablation of polymers: a review. *Polym Int* 2019; 68: 1391–1401.
42. Buls S, Craeghs T, Clijsters S, et al. The influence of a dynamically optimized galvano based laser scanner on the total scan time of SLM parts. In: *24th International Solid freeform fabrication symposium - An Additive Manufacturing Conference, SFF 2013*, 2013, pp.260–266.
43. Penchev P, Dimov S, Bhaduri D, et al. Generic software tool for counteracting the dynamics effects of optical beam delivery systems. *Proc Inst Mech Eng Part B J Eng Manuf* 2017; 231: 48–64.